NASA TN D-526

TECHNICAL NOTE

D-526

CORRELATION OF THE BUCKLING STRENGTH OF PRESSURIZED CYLINDERS IN COMPRESSION OR BENDING WITH STRUCTURAL PARAMETERS

By James P. Peterson

Langley Research Center
Langley Field, Va.

NATIONAL AERONAUTICS AND SPACE ADMINISTRATION
WASHINGTON

October 1960

ERRATA

NASA Technical Note D-526

CORRELATION OF THE BUCKLING STRENGTH OF PRESSURIZED CYLINDERS IN COMPRESSION OR BENDING WITH STRUCTURAL PARAMETERS

By James P. Peterson
October 1960

Equation (A6) (page 10) is an approximation which is good only for small values of N. The "exact" equation for a sinusoidal eccentricity is

$$d\Delta = dN \frac{\lambda}{Et}\left[1 + 6\left(\frac{w}{t}\right)^2 + 6\,\frac{w}{t}\,\frac{N}{t}\,\frac{dw}{dN}\right]$$

When this equation is used to obtain the "tangent" stiffness of a curved strip, the following is obtained in place of equation (All)

$$\frac{Et_e}{Et} = \frac{1}{1 + 6\left(\frac{w_o}{t}\right)^2\left(1 + \frac{12}{\pi^2}\,\frac{N\lambda^2}{Et^3}\right)^{-3}}$$

Use of this equation in constructing figures 2 to 4 leads to results which differ from those obtained with the use of equation (All) by a negligible amount.

NASA-Langley, 1963

Issued 12-18-62

NATIONAL AERONAUTICS AND SPACE ADMINISTR

TECHNICAL NOTE D-526

CORRELATION OF THE BUCKLING STRENGTH OF PRESSURIZED CYLINDERS IN COMPRESSION OR BENDING WITH STRUCTURAL PARAMETERS

By James P. Peterson

SUMMARY

The data on nonpressurized cylinders in bending of NACA TN 3735 and the data on pressurized cylinders in compression and bending of NASA TN D-360 are correlated with structural parameters by using small-deflection buckling theory and reduced values for the extensional stiffness of the cylinder wall. The correlating procedure should prove useful in future shell-buckling investigations by reducing the number of tests required.

INTRODUCTION

The current demand for information regarding the buckling strength of pressurized shells has prompted several recent test programs. (See refs. 1 to 7.) So far the effort has consisted mainly of obtaining test data with little success in interpreting the results of the tests or in correlating the data with known structural parameters. The amount of test data required in such investigations is large and may be considerably reduced if a means for correlating data with shell geometry can be found. A procedure is developed herein whereby the results of some recent cylinder tests are correlated with suitable structural parameters by using small deflection buckling theory and reduced values for the geometric extensional stiffnesses of the cylinder wall. The reduced stiffness values used are devised to provide a basis for correlation where geometric deviations from a perfect cylinder at loss of stability are responsible for the reduced stiffnesses but may also apply where other factors influence the buckling stress.

SYMBOLS

E	Young's modulus, ksi
E_x, E_y	extensional stiffnesses of cylinder wall in axial and circumferential directions, respectively, kips/in.
G	shear modulus, ksi
G_{xy}	shear stiffness of cylinder wall, kips/in.
l	ring spacing, in.
M	moment in plate per inch of width of plate, kips
N	load in plate per inch of width of plate, kips/in.
p	internal pressure, ksi
R	radius of cylinder, in.
s	length measured along arc of imperfection, in. (fig. 5)
t	thickness of cylinder wall, in.
t_e	effective thickness of cylinder wall, in.
w	amplitude of imperfection subjected to a load N, in.
w_o	initial value of amplitude of imperfection, in.
Z	curvature parameter, $\frac{l^2}{Rt}\sqrt{1 - \mu^2}$
$\beta = \frac{w_o^2}{Rt}$	
$\gamma = \frac{\lambda^2}{Rt}$	
Δ	displacement of load, in.
λ	arc length of imperfection, in.
μ	Poisson's ratio

μ'_x, μ'_y Poisson's ratios associated with extension of the cylinder wall in the axial and circumferential directions, respectively

σ normal stress, ksi

σ_{cr} buckling stress, ksi

BUCKLING BEHAVIOR OF COMPRESSION CYLINDERS

A thin-wall cylinder subjected to axial compression usually buckles at a fraction of the predicted buckling load for the cylinder. This discrepancy between theoretical results and test results appears to be largely a function of the radius-thickness ratio of the cylinder and to a lesser extent a function of the structural material, the type of construction, the quality of workmanship, the method of testing, and the size of the test cylinder. The reason for the discrepancy is often attributed to local geometric deviations from the perfect cylinder (so-called imperfections or eccentricities) and to the associated local stress variations which have the effect of rounding off the familiar peak in the theoretical load-shortening curve for a perfect cylinder. The load that a cylinder with imperfections can carry is considerably less than that of a perfect cylinder because the strength of a cylinder depends to a considerable extent on the extensional stiffness of the cylinder wall. Geometric imperfections can cause an apparent reduction in this stiffness because the stretching forces simply tend to increase or decrease the imperfections rather than compress or stretch the fibers of the middle surface of the cylinder wall.

The shape of the cylinder just prior to buckling results to a great extent from the application of the load in the presence of the initial imperfections and, thus, can be expected to resemble the shape of the initial imperfections. Therefore, imperfections resembling the final buckle configuration would be expected to have the greatest deleterious effect since, otherwise, buckling must be accompanied by a change in shape. This phenomenon presumably explains why the discrepancy between theoretical results and test results for cylinders subjected to torsion or circumferential compression is relatively small. The buckles in the natural buckling mode for such cylinders are very long; the buckles are long in the longitudinal direction in the case of circumferential compression, and they are long in an oblique direction in the case of torsion. The likelihood of imperfections of these shapes is not great. On the other hand the theoretical small-deflection buckling load of a cylinder in axial compression is very insensitive to buckle shape; the buckling mode can consist of many small buckles or a fewer number of large buckles. The buckles may be long in the

longitudinal direction or long in the circumferential direction. This characteristic implies that, in compression, imperfections of a variety of shapes and sizes are potentially detrimental.

The buckling behavior of axially compressed cylinders which buckle in the axisymmetric mode appears to be more adequately explained by theory than the behavior of cylinders which buckle in the asymmetric mode. The axisymmetric mode may be obtained by employing cylinders of small radius-thickness ratio or by employing cylinders of larger radius-thickness ratio and internal pressurization. For cylinders with small radius-thickness ratios, it is sometimes difficult to determine whether good agreement with elastic theory is obtained or not; cylinders with radius-thickness ratios small enough to insure axisymmetric buckling are so stable that the buckling stress is at least close to the plastic region of the cylinder material. For cylinders with larger radius-thickness ratios and pressurization, however, axisymmetric buckling can be obtained at very low stress levels; in these instances agreement between theoretical and experimental results may be satisfactory. (See ref. 8.)

CORRELATING PROCEDURE

The small-deflection buckling load of a cylinder in axial compression is strongly influenced by the extensional stiffness of the cylinder wall. This characteristic is exemplified in figure 1 which was constructed from computations based on the stability equation (A4) of reference 9. The curve labeled G_{xy}/Gt in figure 1 was obtained with the assumption that all stiffnesses were held constant at their normal value except G_{xy} which was varied from the normal value Gt to a very small value. The other curve was obtained by three similar but separate calculations - one in which only E_x was varied, one in which only E_y was varied, and one in which G_{xy}, E_x, and E_y were varied simultaneously by the same amount. The computations indicate that the result of a reduced value for any one of the stiffnesses G_{xy}, E_x, or E_y is a reduced buckling load. Furthermore, a reduced value of one of the stiffnesses has about the same deleterious effect on buckling load as a reduced value for all three stiffnesses. Inasmuch as the values for buckling load shown are not independent of Poisson's ratios associated with stretching of the cylinder wall, the values used in the computations for figure 1 are given in table I.

Development of Procedure

The phenomena depicted in figure 1 will be used as the basis of developing a procedure for correlating the data of references 7 and 10 with structural parameters and small deflection theory. For this purpose the local stiffnesses E_x, E_y, and G_{xy} are assumed to be given by

$$\frac{E_x}{Et} = \frac{E_y}{Et} = \frac{G_{xy}}{Gt} = \frac{t_e}{t} \tag{1}$$

where $\frac{t_e}{t}$ is given by equations (A5) and (A11) as developed in the appendix for a curved strip. Equation (A5) applies when the internal pressure is zero and may be rewritten for convenience as follows:

$$\frac{t_e}{t} = \frac{1}{1 + 6\beta \frac{R}{t}} \tag{2}$$

Equation (A11) applies when the internal pressure is not zero and is given by

$$\frac{t_e}{t} = \frac{1}{1 + 6\beta \frac{R}{t} e^{-\frac{24}{\pi^2}\gamma \frac{p}{E}\left(\frac{R}{t}\right)^2}} \tag{3}$$

where

$$\left.\begin{aligned} \beta &= \frac{w_o^2}{Rt} \\ \gamma &= \frac{\lambda^2}{Rt} \end{aligned}\right\} \tag{4}$$

and the load N of equation (A11) is the hoop tensile force of pressurization pR. The indicated form of the parameters β and γ was chosen to give good agreement between the correlating procedure and available test data for constant numerical values of the parameters. Additional data may indicate a better form.

The sweeping assumptions inferred by equations (1) to (3) can be justified only by the end result; that is, on the correlation achieved and not on the merit of the various assumptions involved. However,

some discussion of the assumptions seems warranted. The assumption that E_x, E_y, and G_{xy} can be expressed by a single equation (eq. (1)) is made for convenience since figure 1 indicates that cylinder strength is relatively independent of whether a single stiffness is reduced or whether all three stiffnesses are reduced simultaneously. With this assumption, the local buckling stress of compression cylinders is given by the familiar stability equation for isotropic cylinders in compression with the curvature parameter Z in the stability equation multiplied by $\sqrt{\frac{t_e}{t}}$. For the case of moderately long compression cylinders, the local buckling stress becomes

$$\sigma_{cr} = \sqrt{\frac{t_e}{t}} \frac{E}{\sqrt{3(1 - \mu^2)}} \frac{t}{R} \tag{5}$$

The use of equations (2) and (3) to represent the local extensional stiffness of the wall of a compression cylinder just prior to loss of stability implies that the major effect of geometric imperfections is taken into account by substituting for the small-deflection strain-displacement equations, equations which account for the fact that displacement can occur that does not involve straining of the middle surface of the shell if imperfections are present. The equations for a curved strip are used in place of the corresponding equations for a three-dimensional bulge for simplicity; the essential character of the resulting equations should be somewhat the same. The actual magnitude of the stiffness (that is, the numerical value of β and γ at loss of stability) is established empirically in the following section of this paper.

Application of Procedure

Nonpressurized cylinders in bending.- The bending test results of reference 10 and the nonpressurized bending test results of reference 7 are compared with equation (5) in figure 2. The two sets of data were obtained on similar specimens under similar conditions so the same value of β should apply for either set. The lower limit of the data is predicted fairly well by using $\beta = 0.00065$; the average of the data is given by $\beta = 0.00030$. In either case a single value of β appears to apply over the entire range of data.

Pressurized cylinders in compression or bending.- The data of reference 7 are presented in figures 3 and 4 as $\frac{\sigma}{E}\frac{R}{t}$ plotted against $\frac{p}{E}\left(\frac{R}{t}\right)^2$.

Calculated curves based on equation (5) are also given. The curves were drawn by using the numerical values for the parameters β and γ as follows:

Type test	β	γ
Compression	0.00065	1.2
Bending	.00030	3.6

The value of β for the bending tests was taken from figure 2 as being representative of the middle of the scatter band for those cylinders. A correspondingly reliable value of β is not available for the compression cylinder tests because the number of nonpressurized tests on the type of specimens reported in references 7 and 10 is few. The value $\beta = 0.00065$ for the compression tests was chosen to yield buckling stresses which are in reasonable agreement with the data of figure 3 and, at the same time, conform with commonly observed ratios of compression buckling stress to bending buckling stress.

The values $\gamma = 1.2$ and $\gamma = 3.6$ were chosen to give good correlation between the procedure and the middle of the scatter band of the data of figures 3 and 4 at intermediate values of internal pressure. The data on cylinders with small values of the curvature parameter Z were given less weight in making the choice than data on cylinders with larger values of Z. The buckling data on cylinders in bending at high values of internal pressure were disregarded in choosing a value of γ; however, the data corresponding to strain reversal were considered. (See refs. 7 and 8.)

Figures 3 and 4 indicate that the stabilizing effect of internal pressure is predicted rather well by the correlating procedure; and that, at least for the limited data used, reasonable agreement between the results of the correlating procedure and experiment can be obtained with the use of a single value of γ for a test series. A correlation of the data of references 1 to 6 is not attempted herein. These data evidently have influencing factors, such as plasticity, type of test, and so forth, that did not influence the tests of reference 7. (See discussion in ref. 7.) These factors should be evaluated before attempting to correlate the results of these tests.

Discussion

The correlation achieved in figures 3 and 4 suggests that initial imperfections play an important role in the behavior of cylinders at low values of internal pressure; whereas at high values of internal pressure, any detrimental imperfections that might have existed prior

to pressurization are pulled out by the pressurization stresses so that they play a lesser role. The pressurization stresses themselves create radial prebuckling deformations or imperfections. These deformations are apparently such that they are not very detrimental as far as initiating asymmetric buckling is concerned. Otherwise pressurization might have a destabilizing effect rather than a stabilizing effect. The prebuckling deformations caused by pressurization are such that the effective extensional stiffness of the cylinder wall in the longitudinal direction should be decreased. For this case asymmetric buckles ordinarily would tend to be long in the axial direction and short in the circumferential direction. The prebuckling deformations are the opposite of this; that is, they are short in the axial direction and long in the circumferential direction, and perhaps not very influential in initiating asymmetric buckling. This argument would seem to be strengthened by the fact that the asymmetric buckles which finally appear when a highly pressurized cylinder is loaded to large values of shortening have about the same axial wave length as the axisymmetric prebuckling deformations which they replace.

The correlation achieved in figures 2 to 4 indicates that changes in buckling coefficient with changes in radius-thickness ratio of nonpressurized cylinders as well as the stabilizing effect of pressurization in pressurized cylinders is predicted rather well by the correlating procedure. The procedure should therefore prove useful in eliminating the need for much of the experimental data that are ordinarily required in the establishment of design curves for a new structural material, for a new method of construction, or for a different method of loading. It can be particularly useful in cases where the effect of pressure stabilization is desired on cylinders having proportions such that a single cylinder cannot be used for obtaining data at more than one value of internal pressure.

CONCLUDING REMARKS

A procedure is presented whereby the results of recent cylinder tests are correlated with structural parameters by using small deflection buckling theory and reduced values for the extensional stiffness of the cylinder wall. Values of the reduced stiffness were devised on the basis that geometric imperfections may cause substantial reductions in the effective extensional stiffness of the cylinder wall which, in turn, may cause substantial reductions in cylinder strength. The correlating procedure may be useful in future experimental investigations by eliminating the need for much of the data that is ordinarily required to establish empirical design curves.

Langley Research Center,
National Aeronautics and Space Administration,
Langley Field, Va., July 19, 1960.

APPENDIX

DETERMINATION OF THE STIFFNESS OF A CURVED STRIP

The stiffness of a strip as shown in figure 5 with an eccentricity w_o and subjected to the action of the loads N is desired. It will be obtained by Castigliano's theorem which states that the displacement of the load Δ is related to the strain energy of the strip according to the formula

$$\Delta = \frac{\partial}{\partial N}\left(\int_0^{\lambda} \frac{M^2 ds}{2E\,\frac{t^3}{12}} + \int_0^{\lambda} \frac{\sigma^2 t\, ds}{2E}\right) \tag{A1}$$

The internal bending moments M and middle-plane stresses σ required for equilibrium are

$$M = Ny \tag{A2}$$

and

$$\sigma = \frac{N}{t}\cos \phi \tag{A3}$$

The symbols y and ϕ are defined by figure 5.

When equations (A2) and (A3) are substituted into equation (A1) and the indicated differentiation performed, the stiffness Et_e can be written after some simplification as

$$Et_e = \frac{N}{\Delta/\lambda} = \frac{Et}{\int_0^{\lambda} \frac{\cos^2 \phi\, ds}{\lambda} + \frac{1}{\lambda}\int_0^{\lambda} \frac{y^2 t\, ds}{\frac{t^3}{12}}} \tag{A4}$$

The two terms in the denominator of the right side of equation (A4) can be approximated reasonably well with rather simple expressions. The first term is essentially unity for shallow eccentricities of the type of interest here, and the second term will be recognized as the ratio of the moment of inertia of the curved strip about the line x-x (fig. 5) to the moment of inertia of a flat strip. This term can be

approximated closely by $6\left(\frac{w_o}{t}\right)^2$. With the use of these simplifications, the effective stiffness can be written in terms of the eccentricity w_o as

$$\frac{Et_e}{Et} = \frac{1}{1 + 6\left(\frac{w_o}{t}\right)^2} \tag{A5}$$

Equation (A5) gives the initial stiffness of the strip. That is, it gives the stiffness of the strip as the load N approaches zero, hence the subscript o on w. For this case ($N \to 0$), the stiffness depends mainly (according to eq. (A5) depends completely) on the depth of eccentricity w_o and is relatively independent of the length or shape of the eccentricity. Actually the stiffness is not completely independent of these characteristics but equation (A5) neglects these effects.

In order to determine the stiffness of the strip (fig. 5) as a function of load, further considerations are necessary. As the load N is increased, the eccentricity w_o will be reduced and the stiffness Et_e will be increased. For very large loads the stiffness Et_e will approach Et. The equation expressing the behavior of the strip subjected to an incremental load dN is

$$d\Delta = dN\,\frac{\lambda}{Et_e} = dN\,\frac{\lambda}{Et}\,\frac{t}{t_e} = dN\,\frac{\lambda}{Et}\left[1 + 6\left(\frac{w}{t}\right)^2\right] \tag{A6}$$

where w is the instantaneous value of eccentricity depth, not the initial value. The displacement Δ is the result of a geometric change in shape of the eccentricity and a stretching of the fibers of the strip which can be expressed in equation form, by assuming a sinusoidal eccentricity, as

$$\Delta = \frac{\pi^2}{4\lambda}\left(w_o^2 - w^2\right) + \frac{N\lambda}{Et} \tag{A7}$$

The first term of the right side of equation (A7) gives the displacement resulting from a geometric change in shape of the eccentricity from one with an amplitude of w_o to a more shallow one with an amplitude of w. The last term gives the displacement resulting from a stretching of the middle surface fibers of the eccentricity. Equations (A7) can be rewritten as

$$\left(\frac{w}{t}\right)^2 = \left(\frac{w_o}{t}\right)^2 - \frac{4\lambda\Delta}{\pi^2 t^2} + \frac{4N\lambda^2}{\pi^2 E t^3} \tag{A8}$$

The substitution of equation (A8) into equation (A6) yields the desired differential equation

$$d\Delta = \frac{\lambda}{Et}\, dN\left[1 + 6\left(\frac{w_o}{t}\right)^2 - \frac{24\lambda}{\pi^2 t^2}\,\Delta + \frac{24N\lambda^2}{\pi^2 E t^3}\right] \tag{A9}$$

The solution of equation (A9) for the boundary condition $\Delta = 0$ when $N = 0$ is

$$\frac{4\lambda\Delta}{\pi^2 t^2} = \left(\frac{w_o}{t}\right)^2\left(1 - e^{-\frac{24N\lambda^2}{\pi^2 E t^3}}\right) + \frac{4N\lambda^2}{\pi^2 E t^3} \tag{A10}$$

A comparison of equation (A10) with equation (A8) yields

$$\left(\frac{w}{t}\right)^2 = \left(\frac{w_o}{t}\right)^2 e^{-\frac{24N\lambda^2}{\pi^2 E t^3}}$$

or

$$\frac{Et_e}{Et} = \frac{1}{1 + 6\left(\frac{w_o}{t}\right)^2 e^{-\frac{24N\lambda^2}{\pi^2 E t^3}}} \tag{A11}$$

Equations (A5) and (A11) are used in the body of this paper to affect a correlation between data and theory for nonpressurized and pressurized cylinders, respectively.

REFERENCES

1. Lo, Hsu, Crate, Harold, and Schwartz, Edward B.: Buckling of Thin-Walled Cylinder Under Axial Compression and Internal Pressure. NACA Rep. 1027, 1951. (Supersedes NACA TN 2021.)

2. Fung, Y. C., and Sechler, E. E.: Buckling of Thin-Walled Circular Cylinders Under Axial Compression and Internal Pressure. Jour. Aero. Sci., vol. 24, no. 5, May 1957, pp. 351-356.

3. Harris, Leonard A., Suer, Herbert S., Skene, William T., and Benjamin, Roland J.: The Stability of Thin-Walled Unstiffened Circular Cylinders Under Axial Compression Including the Effects of Internal Pressure. Jour. Aero. Sci., vol. 24, no. 8, Aug. 1957, pp. 587-596.

4. Suer, Herbert S., Harris, Leonard A., Skene, William T., and Benjamin, Roland J.: The Bending Stability of Thin-Walled Unstiffened Circular Cylinders Including the Effects of Internal Pressure. Jour. Aero. Sci., vol. 25, no. 5, May 1958, pp. 281-287.

5. Connor, Jerome J., Jr.: Buckling Characteristics of Circumferentially Reinforced Thin Cylindrical Shells Subjected to Axial Compression and Internal Pressure. Rep. No. WAL TR 715/2, Watertown Arsenal Labs. (Watertown, Mass.), Aug. 1958.

6. Lofblad, Robert P., Jr.: Elastic Stability of Thin-Walled Cylinders and Cones With Internal Pressure Under Axial Compression. Tech. Rep. 25-29 (Contract No. Nonr-1841(22)), Aeroelastic and Structures Res. Lab., M.I.T., May 1959.

7. Dow, Marvin B., and Peterson, James P.: Bending and Compression Tests of Pressurized Ring-Stiffened Cylinders. NASA TN D-360, 1960.

8. Peterson, James P., and Dow, Marvin B.: Structural Behavior of Pressurized, Ring-Stiffened, Thin-Wall Cylinders Subjected to Axial Compression. NASA TN D-506, 1960.

9. Stein, Manuel, and Mayers, J.: Compressive Buckling of Simply Supported Curved Plates and Cylinders of Sandwich Construction. NACA TN 2601, 1952.

10. Peterson, James P.: Bending Tests of Ring-Stiffened Circular Cylinders. NACA TN 3735, 1956.

TABLE I

VALUES USED IN THE CALCULATIONS OF FIGURE 1 FOR POISSON'S RATIOS ASSOCIATED WITH STRETCHING OF CYLINDER WALL

[Poisson's ratio μ was taken to be 0.30 in calculations requiring a numerical value]

Calculation	$\frac{\mu'_x}{\mu}$	$\frac{\mu'_y}{\mu}$
$\frac{E_x}{Et} \leq 1$	$\frac{E_x}{Et}$	1.0
$\frac{E_y}{Et} \leq 1$	1.0	$\frac{E_y}{Et}$
$\frac{G_{xy}}{Gt} \leq 1$	1.0	1.0
$\frac{E_x}{Et} = \frac{E_y}{Et} = \frac{G_{xy}}{Gt} \leq 1$	1.0	1.0

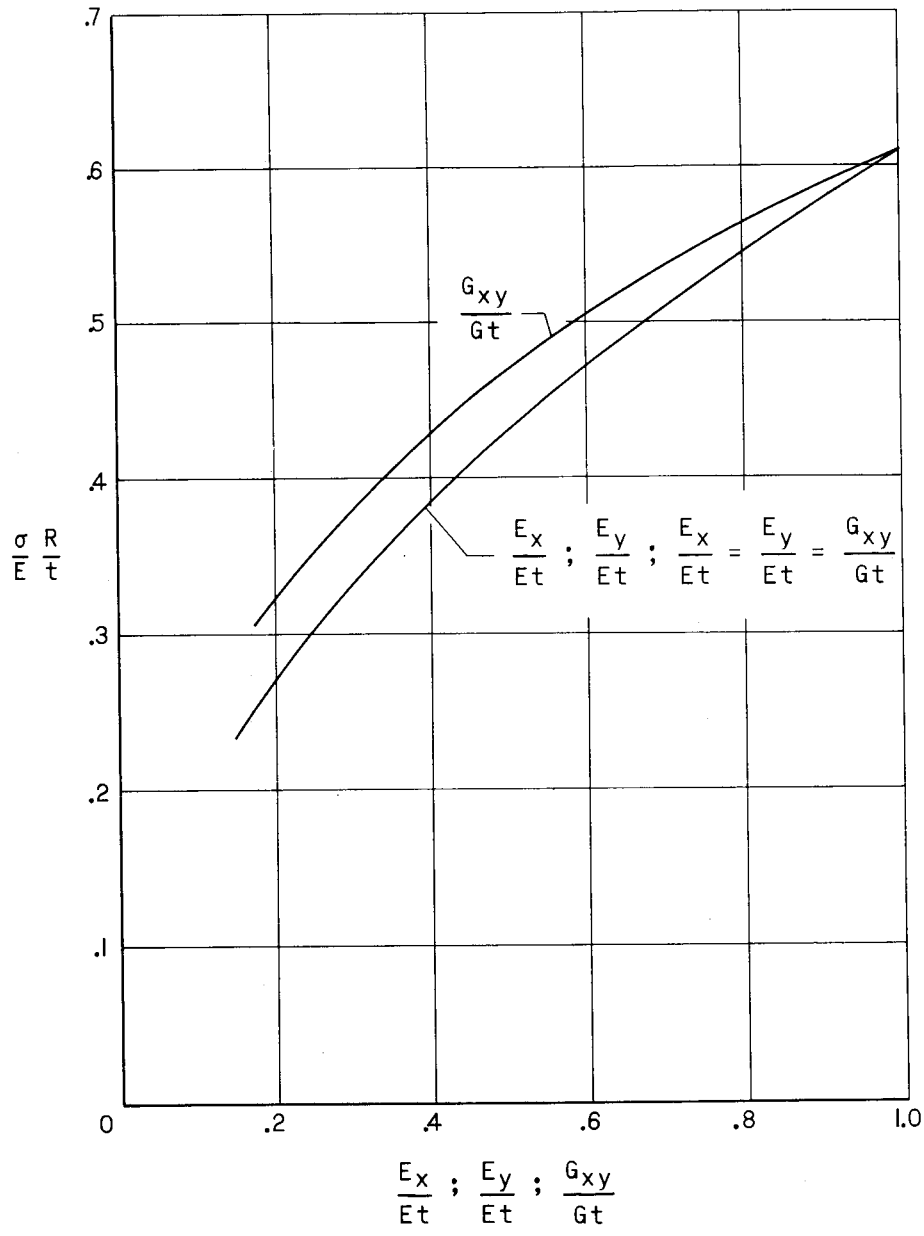

Figure 1.- Effect of reduced values for extensional stiffnesses on the buckling strength of compression cylinders.

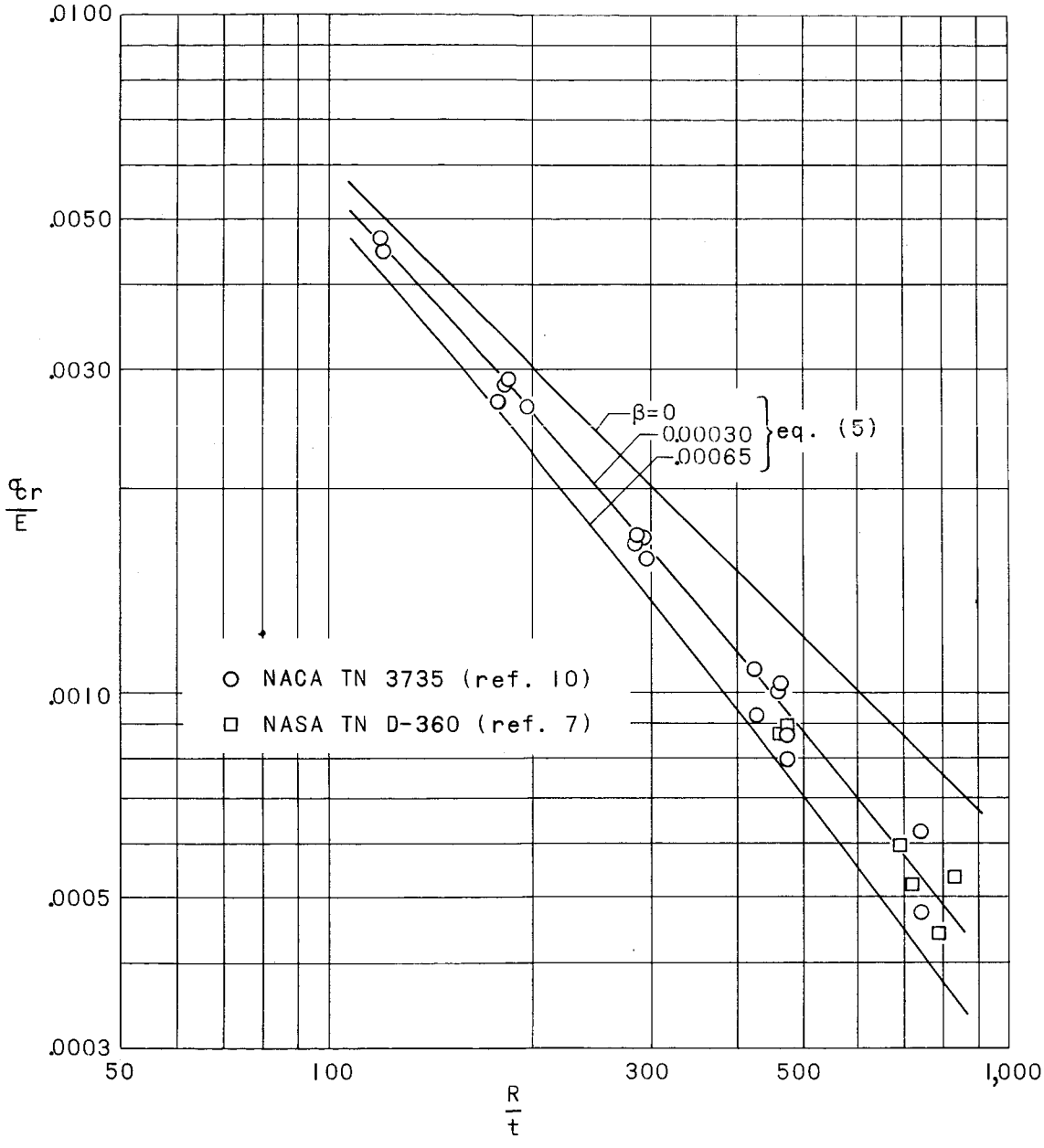

Figure 2.- Application of correlating procedure to nonpressurized bending tests.

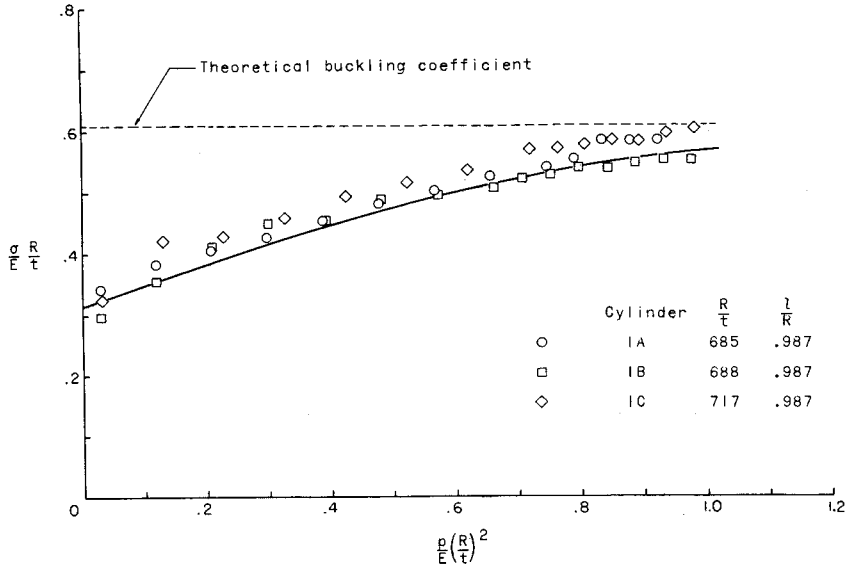

(a) Cylinder 1.

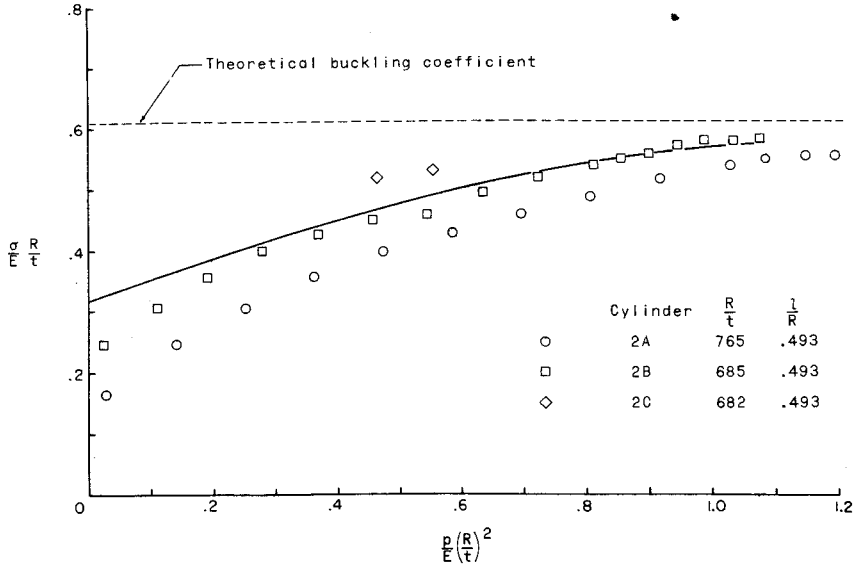

(b) Cylinder 2.

Figure 3.- Application of correlating procedure to pressurized compression cylinders of reference 7.

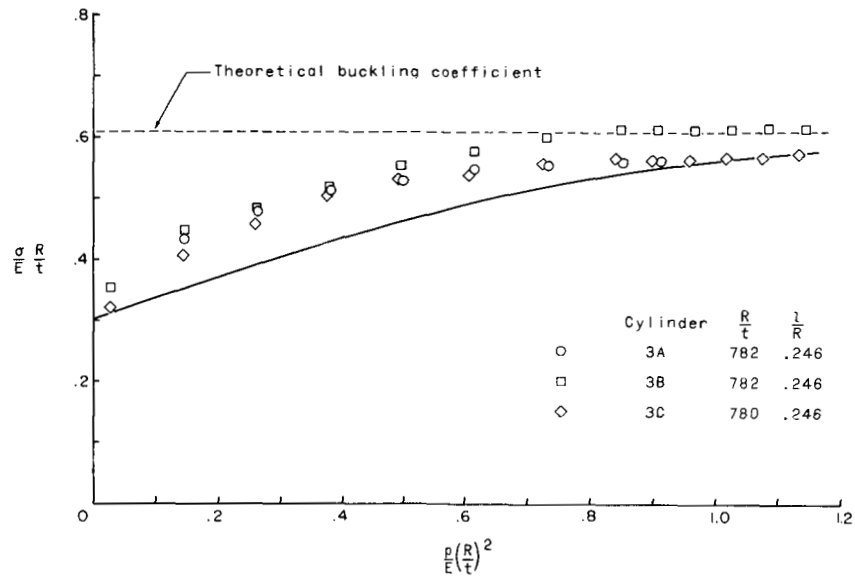

(c) Cylinder 3.

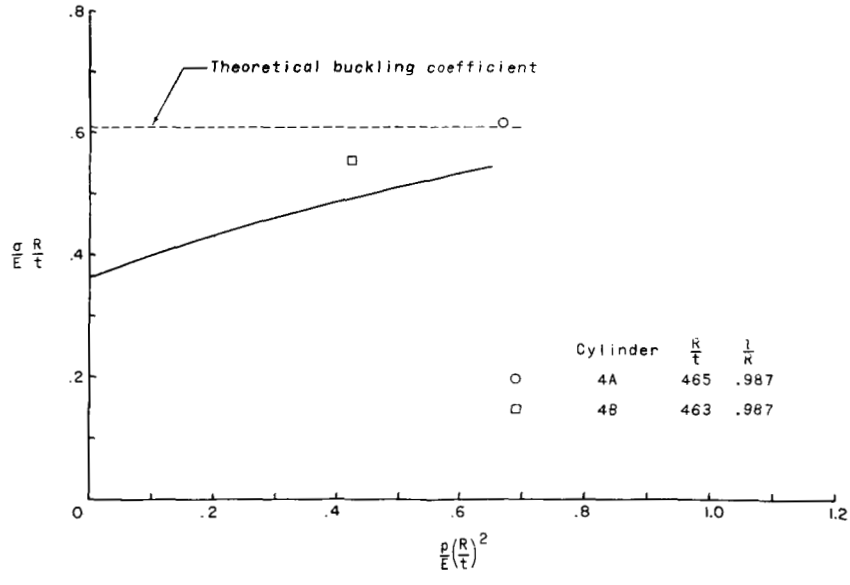

(d) Cylinder 4.

Figure 3.- Concluded.

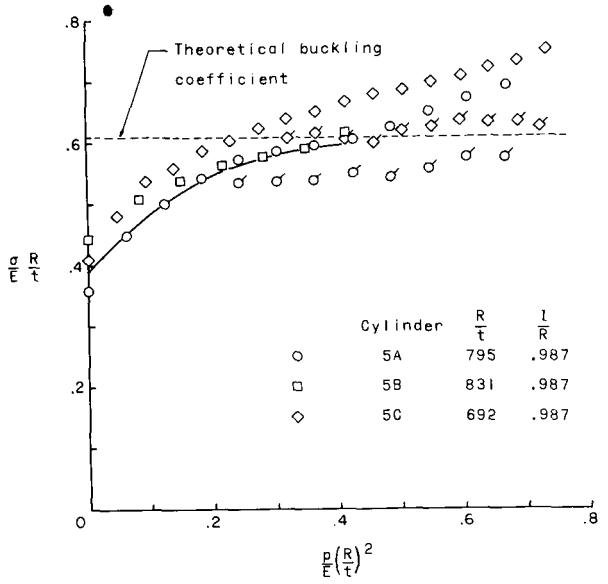

(a) Cylinder 5.

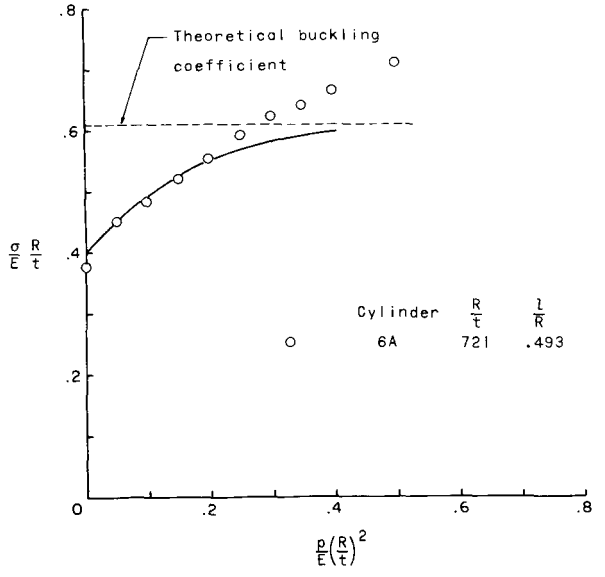

(b) Cylinder 6A.

Figure 4.- Application of correlating procedure to pressurized bending cylinders of reference 7. Symbols with tails denote strain-reversal stresses.

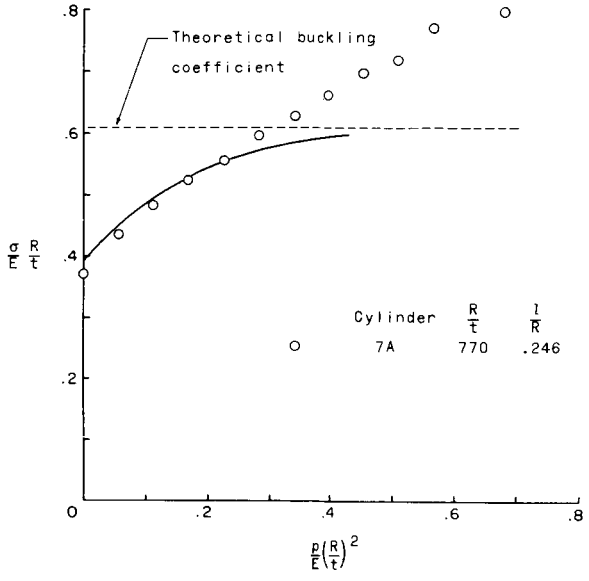

(c) Cylinder 7A.

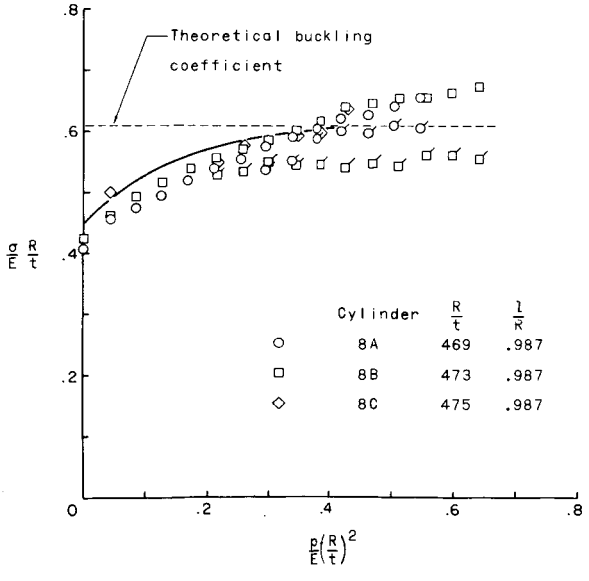

(d) Cylinder 8.

Figure 4.- Continued.

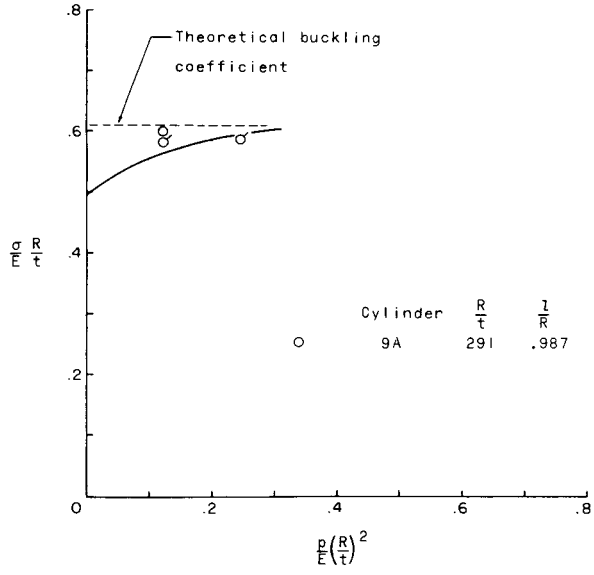

(e) Cylinder 9A.

Figure 4.- Concluded.

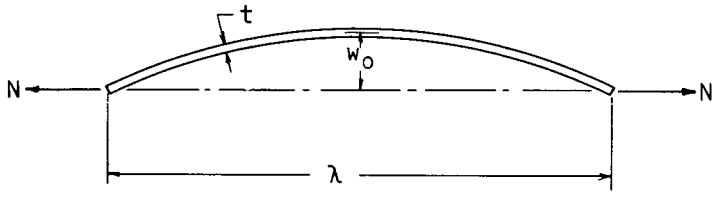

(a) Dimensions.

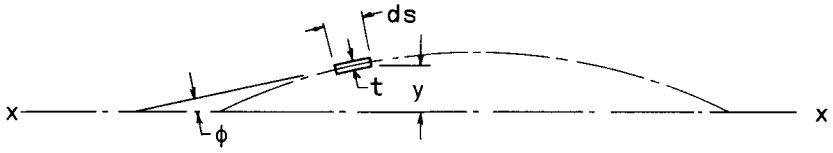

(b) Differential element.

Figure 5.- Dimensions of curved strip.